NASA project

Kees Kroep 4246373

August 10, 2016

Abstract

Type an abstract

Contents

Introduction

This document is a feasability study of a lidar sensor designed for the Europa Clipper. The main focus of this document will lie on the three most challenging aspects of the sensor design. How to achieve the target precision goals of the two modus of operation within the power budget, and the effect of radiation on the system.

First the requirements will be stated in section 1.1, next the assumptions used for this study will be listed in ??, then the feasability of the Altimetry Mode and Hazard Detection Mode will be investigated in ?? and ?? respectively. Section ?? will zoom into the effect of radiation on the system, and finally ?? and ?? will conclude the system with a spec sheet etc...

1 Requirements and Specifications

1.1 High level specifications

The radiation and mass, power and volume budget are listed in table 1 and table 2.

Table 1: Overview of radiation limitations

Radiation	
Total Integrated Dose in Silicon behind 100 mil Al spherical shell	500 krad

Table 2: Requirements for mass, power and volume

Mass, Power & Volume Budget	
Optical Head	<5 kg
Inside vault	<1 kg
Max cable length between optical head and electronics	2 m
Power	<50 W

The Lidar sensor features two operation modes: the Altimetry Mode, and the Hazard Detection Mode.

1.2 Altimetry Mode

Altimetry Mode is the first phase of the landing. During the Altimetry Mode, the Lidar sensor has to provide the altitude of the sensor in relationship to the surface op Europa. The requirements for the Altimetry Mode are listed in table 3

Table 3: Requirements for Altimetry Mode

Altimetry Mode	Threshold	Goal
Max acquisition Slant Range	5 km	8 km
Range Accuracy (3-sigma)	1%	0.10%
Update Rate	0.1 Hz	1 Hz

1.3 Hazard Detection Mode

During the Hazard Detection Mode a 3d map of the surface of Europa must be created around the landing place. The Hazard Mode is operational when the sensor is close enough to the surface of Europa. The requirements for the Hazard Detection Mode can be found in table 4

Table 4: Requirements for Hazard Detection Mode

Hazard Detection Mode	Threshold	Goal
Max range (altitude)	400 m	500 m
Min Operational Range (altitude)	5 m	1 m
Range Accurcay (3-sigma on final 3D map)	10 cm	5 cm
Ground Sample Distance (per pixel on 3D map)	10 cm	5 cm
Ground Area Coverage at max altitude	100 m x 100 m	125 m x 125 m
Time for 3D map creation	1 s	1 s

1.4 Overview

A schematic overview of the sensor is shown in fig. 1.

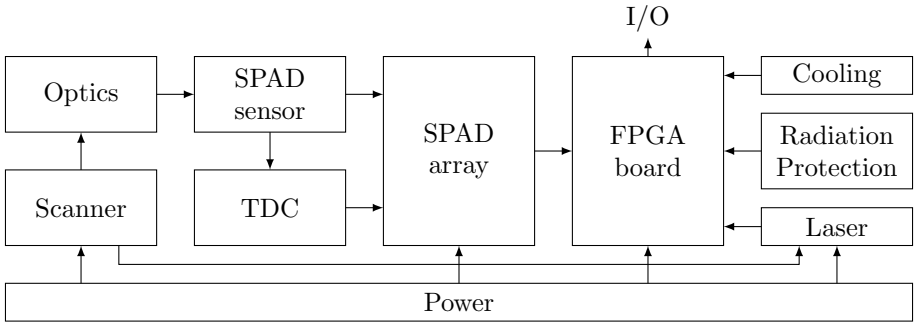

Figure 1: Schematic overview

Laser: The laser must send short pulses but powerful pulses at a predefined frequency, to transmit photons that can be detected by the SPAD Sensor. A critical requirement for the laser is the amount of photons it is able to transmit as a function of time, within the budget and technical limitations.

SPAD Sensor: The Single Photon Avalange Diode (SPAD) is responsible for generating a digital pulse when hit by a photon. A circuit build around the SPAD must ensure that the sPAD is quenched as quickly as possible to minimize the deadline. A critical requirement for the SPAD is a small jitter to maximize the accuracy of the sensor.

TDC: The Time Interval to Digital Converter (TDC) is connected to the laser and the SPAD Sensor. The TDC must measure the time difference between the transmission of teh laser and the receiving at the SPAD sensor. This measurement requires an accuracy of tens of picoseconds to meet the accuracy requirements.

Scanner: The scanner handles the scanning motion that is needed to accumulate the entire picture. Different scanning motions can introduce undesired jitter and heavily influency the amount of SPAD Sensors that are needed on teh SPAD Array.

SPAD Array: The SPAD Array integrates the SPAD Sensors on a chip and connects them to the TDC's. The layout of the SPAD Array is closely rtelated to the scanning motion that is used in the scanner.

Optics: The optics must tranfer as much of the incomming photons as possible to the sensitive area on the SPAD Sensors. The Optics part also implements a bandpass filter around the

target frequency.

FPGA Board: The FPGA Board controls the sensor. It is responsible for accumulating and interpreting the measurements from the TDC's, and controlling the Scanner and Laser.

Cooling: The cooling has to keep the temperature of the FPGA chip under a threshold temperature.

Radiation Protection: The Radiation Protection shields sensitive parts of the sensor from radiation. The most sensitive part of the system is expected to be the FPGA Board, based on experience.

Power: The power block has to supply the scanner, SPAD Array, FPGA Board, and the laser with the required power. The power block has to operate within the specified power budget.

1.5 Assumptions

This section will list the assumption that are made throughout the design.

Reflectivity of surface Europa: It is assumed that out of all light that hit's Europa, 35% is reflected in a perfectly diffuse manner. The rest of the light is either reflected in a specular way that will not hit the sensor, or absorbed by the ice on the surface of Europa. This assumption is made in order to avoid the added complexity when using a more elaborate model.

Wavelength laser: The wavelength of light emitted by the laser is assumed to be $850\,nm$. This wavelength is a typcial choice for Silicon SPAD's.

Bandpass filter:A bandpass filter will be used o filter background noise. This filter is assumed to be a bandpass filter with a center frequency of $850\,nm$ and a FWHM of $10\,nm$.The minimum transmission of the filter is 50%. These values are directly taken from the "*850nm, 10nm FWHM, 12.5mm Mounted Diameter*" product made by Edmund Optics and sold for $75\,\$$.

Jitter of SPAD Sensor: The jitter of the SPAD Sensor, or Full Width Half Max (FWHM) is assumed to be $100\,ps$. This value is a typical FWHM for state of the art Silicon SPAD's.

Jitter of TDC: The jitter of the TDC's is assumed to be insignificant when compared to the jitter of $100\,ps$ caused by the SPAD Sensors. Experience with previous designs show that TDC jitter is generally a very small contributor to overall jitter.

Accuracy of TDC: The accuracy of the TDC is assumed to be $50\,ps$, and therefore well within the accuracy requirements. The accuracy should be $5\,cm$. Using eq. (1), the desired accuracy is $333\,ps$.

$$t = \frac{2x}{c} \tag{1}$$

where x is the accuracy in distance, and $c \approx 3 \cdot 10^8$ the speed of light. The factor two is present because the light travels the distance twice.

Sunlight: It is assumed that the light from the sun that is reflected of Europa is the only signifant contributor to background noise. No other sources of light will be considered.

Photon Detection Probability: It is assumed that the PDP of the SPADs is 35%.

Effective area on chip: It is assumed that 5% of the SPAD Array can be used to receive photons. This assumption is based on current gen Silicon SPAD's.

Laser light hitting target: It is assumed that all the light that leaves the laser is hitting the target area on Europa.

Signal to Noise Background Ratio: It is assumed that a Signal to Noise Background Ratio (SNBR) of 0 dB will be sufficient for the sensor. This value is based on previous research on Silicon SPADs.

Laser efficiency: It is assumed that the laser has an efficiency of 10%.

Surface of SPAD: It is assumed that the surface of a single SPAD is $20 \times 20\,\mu m^2$.

2 Altimetry Mode

The Altimetry Mode is the mode in which only the altitude of the device in relationship to Europa is required. The main challenges for the altimetry mode are acquiring the required resolution, acquiring the required speed, staying within the power budget, and being sufficiently resilient against the accumulated radiation for the entire trip.

The first step will be to create a model of the noise that will be present at Europa. Then the required amount of signal will be calculated, resulting in the required signal power.

2.1 Optics

The receiver optics are a good place to start of with, beacuse the optics are not very dependent on results attachieved in other areas. The optics have to transport as many desired photons, and as little unwanted photons to the active area on the SPADs as possible. All while having an acceptable depth of field.

The most basic solution is a single lens with an aperture. The opacity of the lens can be calculated with the absorption of the lens material and f-number of the lens using eq. (2).

$$\text{opacity} = \frac{1 - \text{absorption}}{\text{f-number}^2} \tag{2}$$

The performance of a possible configuration is shown in table 5

Table 5: Performance of basic optics solution

Basic Optics	
f-number	2.00
absorption	5.00 %
opacity	23.75 %

Improvements

There are a couple of additions that can improve the performance of the optics. The first and very necessary one, is the use of a bandpass filter. The transmitted signal will have a very specific bandwidth of $850\,nm$. Using a narrow bandpass filter one can filter out an enormous part of the background noise. The filter will have an opacity of 50 % for the target wavelength.

The captured photons that hit the lens need to be guided to the active area of the SPADs. If the active area on the chip is very small, one can use microlenses to improve the effectiveness of the optics. A Microlens focusses light on a single SPAD on the chip. Two types of microlenses

will be considered: a spherical lens, and a square shaped lens. The presence of microlenses poses a limitation of the main lens. The f-number must be relatively large. A higher f-number means a smaller aperture and therefore more loss of photons. A way of dealing with this problem is to use a second lens instead. An overview of the available options is shown in fig. 2

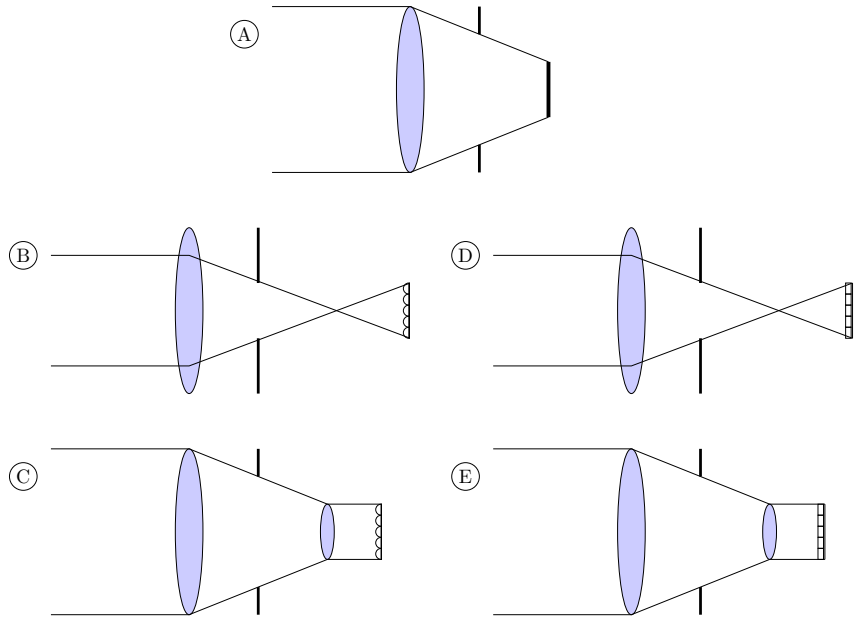

Figure 2: Overview of possible receiver optics implementations

$$\text{opacity} = (1 - \text{absorption}_1)(1 - \text{absorption}_2) \cdot \text{opacity filter} \cdot \frac{X}{\text{f-number}^2} \tag{3}$$

Where X is the active area on the chip. A comparison between the different options is shown in table 6

Table 6: comparison of different optics solutions

Type	**A**	**B**	**C**	**D**	**E**
absorption 1^{st} lens	0.05	0.05	0.05	0.05	0.05
f-number	2	8	2	8	2
absorption 2^{nd} lens	0	0	0.05	0	0.05
opacity bandpass filter	0.5	0.5	0.5	0.5	0.5
active area on chip	X	0.55	0.55	0.65	0.65
effective opacity	$X \cdot 11.75\,\%$	$0.4082\,\%$	$6.204\,\%$	$0.4924\,\%$	$14.6656\,\%$

The comparison in table 6 shows some good alternatives to the basic lens, if there is a need for it due to a small active area on the chip. However, most of the future calculations will focus on the basic model A.

2.2 Noise caused by the sun

The sun is the most dominant source of unwanted photons at Europa. This section will investigate how much energy is hitting the surface of Europa.

To calculate that the sun will be modelled as an ideal black body. The spectral irradiance of the sun can be calculated using eq. (4).

$$I_\lambda(\lambda, T) = \frac{2hc^2}{\lambda^5} \frac{1}{e^{\frac{hc}{\lambda kT}} - 1} \tag{4}$$

where $I_\lambda(v, t)$ is spectral irradiance with unit W/m^3.
h is the planck constant
c is the speed of light in vacuum
k is the Boltzman constant
λ is the wavelength of the electromagnetic radiation
T is the absolute temperature of the body

The spectral irradiance of the sun is calculated in table 7.

Table 7: Calculation of sun irradiation

Sun irradiation	
h	$6.63 \cdot 10^{-34}\, Js$
c	$3.00 \cdot 10^{8}\, m/s$
k	$1.38 \cdot 10^{-23}\, j/K$
λ	$850.00\, nm$
T	$5.78\, kK$
I_λ	$1.51 \cdot 10^{4}\, W/m^2/nm$

The next step is to calculate the power emitted by the sun in the specified bandwidth, at the location of Europa. The specified bandwidth is in this case the assumed bandpass filter used on the lens. The emitted power is calculated by modelling the sun as a point source, and then spreading that power over a sphere with a radius equal to the distance between the sun and Europa, as is done in eq. (5).

$$P_{sun} = I_{\text{sun}} B_\lambda S \frac{r_{\text{sun}}^2}{r_{\text{europa}}^2} \tag{5}$$

where I_{sun} is the spectral irradiance of the sun at the center frequency of the filter, B_λ is the bandwidth of the filter in meters, S the surface area of the target area on Europa, r_{sun} the of radius of the sun, and r_{europa} the distance between Europa and the sun. The effective radiance of the background noise at Europa is calculated in table 8 using eq. (5).

Table 8: Calculation of background power on target area on Europa

Background power	
I_λ	$1.51 \cdot 10^{13}\, W/M^3$
B_λ	$10.00\, nm$
Surface area	$15625.00\, m^2$
r_{sun}	$6.96 \cdot 10^{5}\, km$
r_{europa}	$7.79 \cdot 10^{8}\, km$
P_B	$1.89\, kW$

The next step is to calculate the percentage of energy that hits the device when hovering over Europa. The focal length and aperture ofthe lens will be configured in such a way that the target surface on Europa fills the entire view at the maximum altitude of the Hazard Detection Mode, so that altitude will be chosen to calculate the received noise power. The amount of power received at the lens of the device can be calculated using eq. (6).

$$P'_B = \frac{P_B \cdot R_{Europa} \cdot D_l \cdot \text{opacity}}{2r^2} \tag{6}$$

where P'_B is the power hitting the lens,
P_B the noise power on the target area of Europa,
R_{Europa} the reflectivity of Europa,
D_l the diameter of the lens,
opacity the opacity of the lens,
and r the altitude of the device. The calculations are performed in table 9.

Table 9: Amount of noise power that hits the SPAD array

noise power at SPADs	
P_B	$1.89\,kW$
r	$500.00\,m$
R_{europa}	$35.00\,\%$
Diameter lens (D_l)	$50.00\,mm$
opacity optics	$11.75\,\%$
P'_B	$7.76\,\mu W$

Finally the power needs to be converted to number of photons. To calculate how many photons bounce from the surface of Europa and actually hit the light. To calculate the amount of photons one needs to know the amount of energy per photon. This can be calculated using eq. (7). The calculation is performed in table 10.

$$E_{photon} = \frac{hc}{\lambda} \tag{7}$$

Table 10: Pulse frequency for both modes of operation

energy of photon	
h	$6.63 \cdot 10^{-34}\,Js$
c	$3.00 \cdot 10^{8}\,m/s$
λ	$850.00\,nm$
E_{photon}	$2.34 \cdot 10^{-19}\,J$

The amout of photons per second can then be calculated using eq. (8). The calculation is shown in

$$\text{photon}/s = \frac{P}{E_{photon}} \tag{8}$$

Table 11: Pulse frequency for both modes of operation

photons hitting SPADs	
P'_B	$7.76 \cdot 10^{-6}\,W$
E_{photon}	$2.34 \cdot 10^{-19}\,J$
photons at SPADs	$3.31 \cdot 10^{13}\,\text{photon}/s$

2.3 Detected photon characterisation

This section tackles the problem of calculating the resolution of the set-up. To do this, the different types of detection by the SPADs, due to sunlight, signal source and dark counts, must be characterized first.

To avoid pileup a couple of temporary assumptions about the performance of the SPADs will be made. Firstly, it is temporarily assumed that the percentage of the surface that is sensitive to photons is 50 %. Secondly it is temporarily assumed that the dark count rate (DCR), of the entire array is $PSS_N = 1 \cdot 10^9 \text{photon}/s$.

The amount of detected sunlight photons detected by the SPADs per second can now be calculated using eq. (9). The calculation are shown in table 12. Both the sunlight detections and the DCR detections are uniformly distributed.

$$PPS_B = \text{photons at SPADs} \cdot \text{PDP} \cdot \text{effective area} \tag{9}$$

Table 12: Amount of detected sunlight photons detected per second

PPS for background photons	
Photons at SPADs	$3.31 \cdot 10^{13}\,\text{photon}/s$
PDP	35.00 %
effective area	50.00 %
PPS_B	$5.80 \cdot 10^{12}\,\text{photon}/s$

The next step is to characterize the relationship between the laser power and the received photons. It is assumed that all light emitted by the laser is hitting Europa. It is also assumed that the efficiency of the laser is 10 %. Next, similar calculation as performed with P_B can be used to calculate the amount of detected signal photons per second PPS_S. There is one important difference however: where for sunlight an altitude of $500\,m$ was used, for the signal photons an altitude of $8\,km$ must be considered. The calculation are performed in table 13. Note that even with the largest power budget of $50\,W$, the SNR will be well below $0\,dB$.

Table 13: Amount of detected signal photons detected per second

PPS for background photons	
P_S	$1.00 \cdot 10^{-1}\,W$
Altitude	$8.00\,km$
P'_S	$1.61 \cdot 10^{-12}\,W$
PPS_S	$1.20 \cdot 10^{6}\,\text{photon}/s$

The signal photons are not uniformly distributed like the noise and background photons. The signal photons are assumed to be distributed in a normal distribution with a $FWHM = 100\,ps$. This distribution is convoluted with the jitter on the SPADs, which is assumed to be a normal distribution with a $FWHM = 100\,ps$. Using eq. (10) and eq. (12), the resulting distribution has a $\sigma_S = 60\,ps$. The mean μ_s is equal to the time of flight of the photon.

$$FWHM = 2\sqrt{2\ln 2}\sigma \tag{10}$$

$$\sigma = \frac{FWHM}{2\sqrt{2\ln 2}} \tag{11}$$

$$\sigma_{f\otimes g} = \sqrt{\sigma_f^2 + \sigma_g^2} \tag{12}$$

The maximum allowable $FWHM$ of the measurement is $333\,ps$ as shown in section 1.5. Using eq. (11) the maximum standard deviation is $\sigma = 141\,ps$.

2.4 Sampling Method

The sampling method used has a massive impact on the performance of the system. This section investigates the options that can be chosen from.

The time that the sensor should listen to a response is determined by the maximum round trip time of a photon, and can be calculated using eq. (13).

$$t_{round} = \frac{2r}{c} \tag{13}$$

where $c \approx 3 \cdot 10^8$ is the speed of light, and r the altitude of the sensor.

The next step is to calculate the relationship between oberved number of good and bad photons for a given listening period, and the resulting standard deviation of the measurement. To calculate the standard deviation of the sum of multiple random variables that are independent and uncorrelated, one can use eq. (14)

$$\mathrm{Var}[aX + bY + cZ] = a^2\mathrm{Var}[X] + b^2\mathrm{Var}[Y] + c^2\mathrm{Var}[Z] \tag{14}$$

Because the DCR and sunlight photons have the same uniform distribution they are taken from the same uniform random variable N, where n is the amount of detected sunlight and dark photons, $\mu_n = \frac{1}{2}t_{round}$, and $\sigma_n = \frac{1}{\sqrt{12}}t_{round}$. The signal photons are taken from the random variable S, where s is the amount of detected signal photons, $\mu_s = ToF$, and $\sigma_s = 42.5\,ps$. The resulting mean μ_{tot} can be calculated using eq. (16). The error with the desired μ can be calculated using eq. (18).

$$\mu_{tot} = \frac{1}{s+n}\Big(\sum_{k=1}^{s}\mu_s + \sum_{l=1}^{n}\mu_n\Big) \tag{15}$$

$$= \frac{s \cdot Tof}{s+n} + \frac{n \cdot \frac{1}{2}t_{round}}{s+n} \tag{16}$$

$$\mu_{\text{error}} = |ToF - \mu_{tot}| \tag{17}$$

$$= \Big|\frac{n(ToF - \frac{1}{2}t_{round})}{s+n}\Big| \tag{18}$$

The resulting standard deviation σ_{tot} can be calculated using eq. (22).

$$\mathrm{Var}_{tot} = \mathrm{Var}\Big[\frac{1}{s+n}\Big(\sum_{k=1}^{s}\mathrm{Var}_s + \sum_{l=1}^{n}\mathrm{Var}_n\Big)\Big] \tag{19}$$

$$= \frac{1}{(s+n)^2}(s\sigma_s^2 + n\sigma_n^2) \tag{20}$$

$$\sigma_{tot} = \sqrt{\mathrm{Var}_{tot}} \tag{21}$$

$$= \frac{\sqrt{s\sigma_s^2 + n\sigma_n^2}}{s+n} \tag{22}$$

Using eq. (22), one can calculate the relationship between the amount of signal photons needed for a given amount of noise photons. For the long distance a $t_{round} = 53.3\,\mu s$ is used. Using eq. (24)

the realtionship between the number of noise photons and required signal photons is shown in fig. 3. Note that the amount of required signal photons first rises quickly, then slowly, and finally even drops. The reason for this trend is that increasing the number of random samples also decreases the standard deviation by itself. Figure 4 shows the same relationship for a smaller number of noise photons.

$$\sigma_{tot} = \frac{\sqrt{s\sigma_s^2 + n\sigma_n^2}}{s+n} \tag{23}$$

$$s = \frac{\sigma_s^2 + \sqrt{\sigma_s^4 - 4\sigma_s^2\sigma_{tot}^2 n + 4\sigma_n^2\sigma_{tot}^2 n} - 2\sigma_{tot}^2 n}{2\sigma_{tot}^2} \tag{24}$$

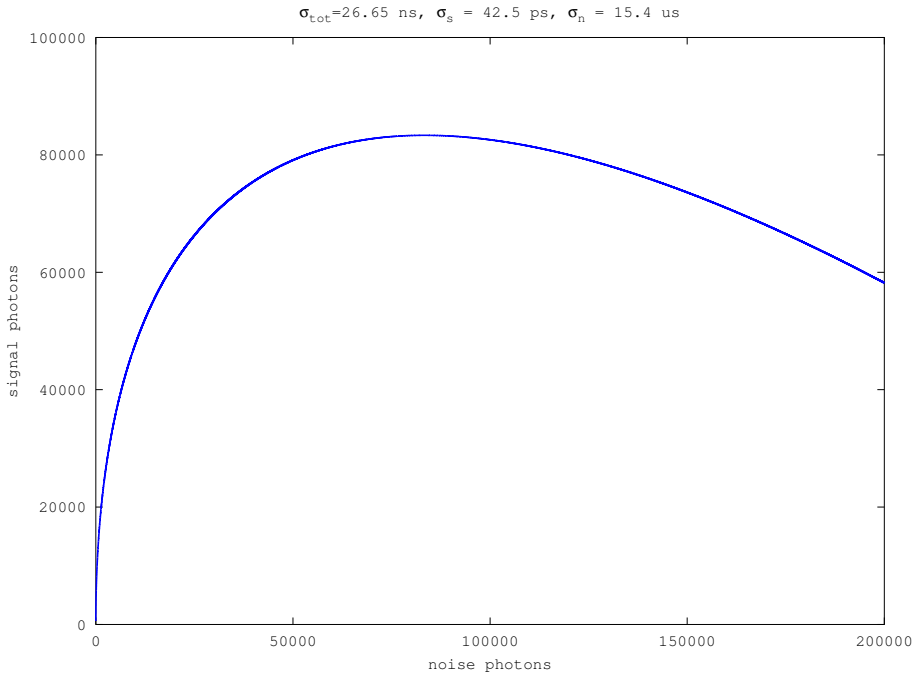

Figure 3: Relationship between number of signal and noise photons to get the required resolution

2.4.1 Energy Threshold

An energy threshold can be a very powerful way to improve signal to noise ratio. The signal photons all arrive with a $FWHM = 100\,ps$, while the noise photons are spread out over $53.3\,\mu s$. An energy threshold is a perfect way to take advantage of this. When the phoons are divided over bins, the expected number of bins can be modelled as Poission process. Using this the efficiency of the energy threshold can be perfomed which is shown in fig. 5, where the opacity is 1 if all photons pass through the threshold, and 0 if no photons pass through the threshold. It is important to notice that a certain threshold has no effect at all if the expected number of photons is sufficiently high. The threshold is most effective when the opcity for the signal photons is close to 1, and the opacity for noise photons close to 0. To apply a threshold however, one needs to assemble a historgram of all the detections. The feasability of such a histogram will be investigated later, but for now both a system with and without an energy threshold are considered.

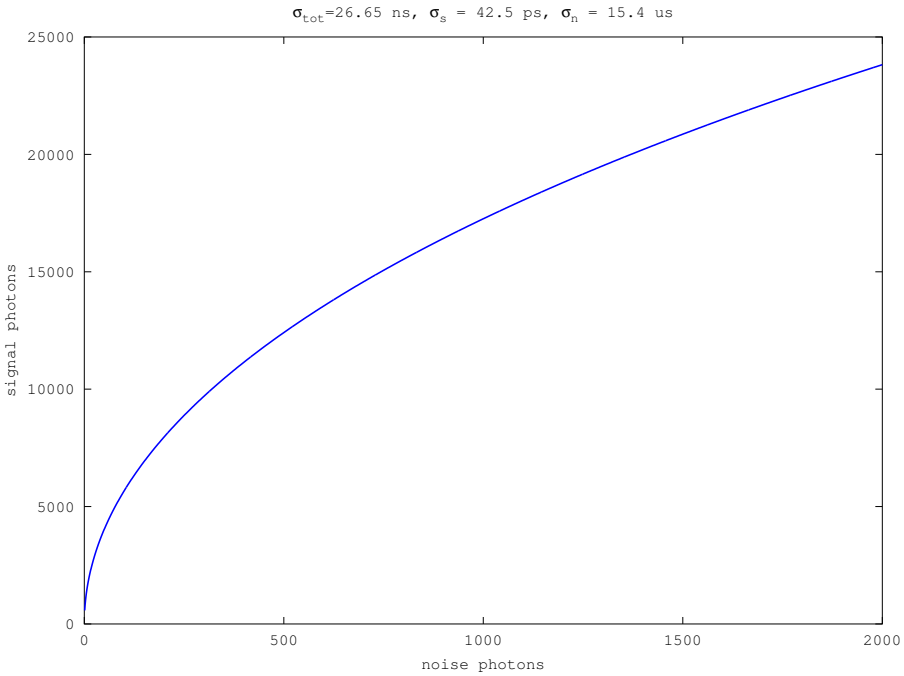

Figure 4: Relationship between number of signal and noise photons to get the required resolution

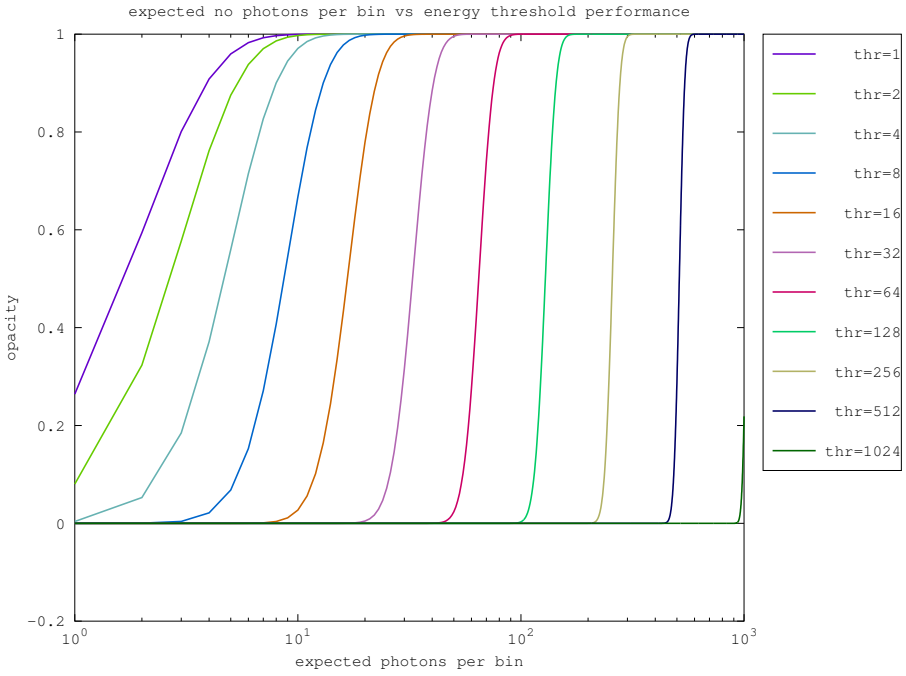

Figure 5: Expected number of photons per bin versus the opacity of the threshold, where opacity=1 means all photons pass through the threshold, and opacity=0 means no photons pass through the threshold

2.5 Required Laser Power

The requirement for the altimetry mode changes based on the height. The target is a resolution of at least 0.1 %. To ensure that this requirement is met, both the largest altitude of $8\,km$, and the smallest altitude of $500\,m$ will be investigated.

The minimum resolution for the largest and shortest altitude are $8\,m$ and $0.5\,m$ respectively. The maximum allowable FWHM can be calculated using eq. (25). Using eq. (11) the maximum standard deviation can be calculated. The calculations are performed in table 14.

$$FWHM_{max} = \frac{2x}{c} \tag{25}$$

Table 14: Pulse frequency for both modes of operation

AM requirements	short	long
altitude	$500\,m$	$8\,km$
resolution	$50\,cm$	$8\,m$
FWHM	$3.33\,ns$	$53.33\,ns$
σ	$1.42\,ns$	$22.65\,ns$

2.5.1 Peak Power

A very important restriction to the sampling method is the highest achievable peak power of the laser. If there would be no limit on the peak power, one could send out one extremely powerful pulse, listen for an extremely short period of time, and then reconstruct the altitude. The key advantage is the listening time. Shortening the listening time directly reduces the amount of background and noise that can be observed.

During the transmission of the laser, the peak power must be more than the average power of the background noise. Using eq. (26) one can calculate the average optical power required for the laser to get an $SNR = 0$. These calculations are performed in table 15. Combing that result with a laser efficiency of 10%, this gives a required electrical power of $4.8\,MW$ to match the power of the sun. In order to be able to distinguish noise from signal, the peak power is lower bound by this amount of power.

$$P_{av} = P_B \frac{\text{HDM altitude}^2}{\text{current altitude}^2} \tag{26}$$

Table 15: required average power to get SNR=0

matching average power	
P_B	$1.89\,kW$
HDM altitude	$500\,m$
current altitude	$8\,km$
P_{av}	$482.78\,kW$

Using the results in fig. 3, and the calculations performed in section 2.3, a relationship between the peak power and average power can be constructed, which is shown in fig. 6. This figure illustrates the clear advantage of having a high peak power. If the peak power is high enough, a single pulse is enough to acquire the desired resolution, resulting in an extremely low average power. The figure also shows that the increase of amount of pulses decreases the required peak power, but after a certain point this decrease is no longer significant. It is important to note that the variation in the mean is not considered here, which means that the actual required power will higher.

When the energy threshold is added a very different relationship can be found. The threshold can be so powerful that noise can be almost completely eliminated without losing any signal photons, as long as the difference between the expected number of signal photons per bin is sufficiently larger than the expected number of noise photons per bin. To avoid pileup, it is assumed that a difference of a factor $F = 4$ will be sufficient. It will also be assumed that a single pulse will be enough to acquire the required information. Using the calculations in table 15, one can quickly tell that the peak optical power must be at least $1.9\,MW$. This is still an enourmous amount of peak power to produce, and hardly feasable.

2.5.2 Reducing the field of view

The limit calculated in table 15 is too high to design feasable laser specifications. The only way to reduce this lower limit, the amount of observed background noise must be further limited. To limit the amount of observed background noise, the field of view must be limited. Until this point the amount of background noise was defined as the amount of noise hitting the device from a $125 \times 125\,m^2$ surface on Europa at an altitude of $500\,m$. This means that on an altitude of $8\,km$, a surface of $2 \times 2\,km$ is obsverved. Now we take a look at what happens when the field of view is limited to a thin slice of $125 \times 0.1\,m^2$. Assuming that the laser is capable of tranmitting exactly into the small target area, this reduces the limit calculated in table 15 by a factor 1250. This shows that the altimetry mode for the laser is feasable, but that a sufficiently limited field of view is required. The target area for the Altimetry Mode can be arbitrarily small. The field of view can be limited by either the lens, or by disabling a portion of the SPADs on the chip.

Figure 6: required peak power for a given average power for the requirements at an altitude of 8 km

3 Hazard Detection Mode

The Hazard Detection Mode is the mode of operation that operates closer to Europa than the Altimetry Mode. The main difference and challenge is however, is that this time a detailed heightmap must be formed. Therefore, for the Hazard Detection Mode, the layout of the SPADs and the scanning method are essential in determining the feasability of the device.

3.1 Types of SPADs

In Hazard Detection Mode, individual SPADs will have the responsibility of measuring their part in the target. Therefore it is important to first investigate what type of SPAD is best suited for the device. As mentioned in section 2.1, SPADs can have microlenses. Two types are considered: conventional spherical lenses, and rectangular lenses. Spherical lenses typically achieve an effective active area of approximately 55 %, while rectangular lenses typically get an effective active area of appeoximately 65 %. The active area can also be shaped in different sizes, and a circular and rectangular shape are considered here. An overview of the different options is shown in fig. 7.

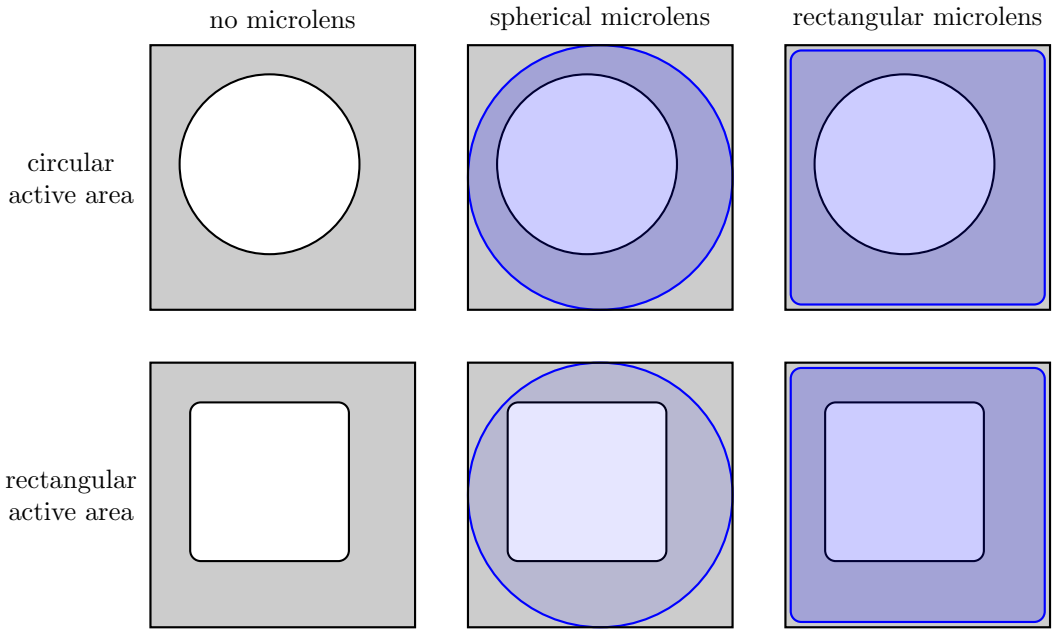

Figure 7: Options for lenzes with varying types of active areas and microlenses

The use of microlenses is not the only viable of option of increasing the active area on the chip. A second option is to pick the circuitry required per SPAD, and push it to the side. These circuitry include the Read-Out Integrated Circuit (ROIC) that also includes the quenching of the SPADs, and the Time interval to Digital converter (TDC).

To avoid pileup, the following calculations are done for an 0.18 μm technology and it is assumed that the ROIC will take up 110 μm^2 surface area per SPAD, and that the TDC will take up 1200 μm^2 surface area per SPAD. It will also be assumed that the minimum amount of pitch between two SPADs is 1.5 μm. These numbers are based on current SPAD designs in 0.18 μm technology. An overview of the performance of all different possibilities is shown in fig. 8.

Figure 8: effective area for different approaches in relationship to the pitch of the SPAD on 0.18 μm technology